A Theoretical Treatment on the Behavior of the Hydrogen-Bonded Proton in Malonaldehyde

Shigeki Kato, Hiroshi Kato, and Kenichi Fukui*

Contribution from the Department of Hydrocarbon Chemistry, Kyoto University, Kyoto, Japan. *Received May 3, 1976*

Abstract: The quantum mechanical behavior of the hydrogen-bonded proton is treated by means of the intrinsic reaction coordinate previously proposed. The reaction coordinate is obtained by the aid of the gradient of potential energy determined by CNDO/2 procedure. The effective motion along the reaction coordinate is calculated considering all vibrational motions perpendicular to the reaction coordinate. The statistical feature of vibrational state of malonaldehyde is discussed on the basis of the canonical ensemble in a heat bath of a given temperature, and the density matrix is calculated in order to examine the proton distribution on the reaction coordinate and the rate of proton transfer with relation to the temperature. An ellipse-like orbit of proton motion is suggested.

The proton moves through the hydrogen bonds in many chemical and biological systems. Both theoretical and experimental chemists have been much interested in such a problem for a long time.[1] On theoretical ground, the detailed description of the proton transfer or exchange in hydrogen bonding systems seems to include two separated steps. The first step is to calculate the potential energy surface for the proton motion. For this purpose, semiempirical and ab initio molecular orbital (MO) calculations have been carried out for a variety of systems including intra- and intermolecular hydrogen bondings.[2] These studies have given encouraging results in predicting the proton potentials as well as the stable geometries, hydrogen bond energies, and spectroscopic properties. The origin of hydrogen bond formation has also been explained by analyzing the binding energy or the charge distribution.[3]

The second problem is to solve the equation of motion for protons on a given potential surface and to evaluate the equilibrium constant or the rate of proton transfer after statistical averaging. Löwdin[4] reviewed the quantum mechanical treatments of proton tunneling in a double well potential of the hydrogen bonding in nucleotide base pairs and discussed them in connection with the biological duplication. Although further developments in this direction of research have been achieved,[5] the greater part of these works has been based on the model or experimentally adjusted empirical potentials.

In order to describe such a process, one has to define the reaction coordinate, the curve leading from the bottom valley of initial state over the transition state to the valley of final state on the potential energy surface, inherent to the system concerned.

In the present paper, we proposed a method to treat the proton exchange in the intramolecular hydrogen bonding system by means of "intrinsic" reaction coordinate[6] and apply it to the enol tautmer of malonaldehyde, which is the simplest 1,3-dione compound. The reaction coordinate is defined by the use of the gradient of the quantum mechanical hypersurface of reacting species and is here obtained by the semiempirical CNDO/2 MO method.[7]

Some MO theoretical studies of malonaldehyde have been presented.[8-10] The position of the proton has been given much attention in these works. Schuster[8] first calculated the potential surface of the proton by the CNDO/2 method. His results predicted that the energy barrier for the proton transfer is quite low (0.5 kcal/mol). Recently ab initio MO procedure has been applied by two groups. Karlström et al.[9] concluded that the stable configuration of this compound is asymmetric and the barrier height is calculated to be 11.5 kcal/mol. Isaacson and Morokuma[10] employed semiempirical (CNDO/2 and INDO) and ab initio calculations on this molecule and proposed the condition for a neutral hydrogen bonding system to have a symmetric configuration. They suggested the possibility of malonaldehyde having a symmetric hydrogen-bonding proton on the basis of their hypothesis.

After our work had been submitted for publication, the microwave study by Rowe, Duerst, and Wilson[11] was presented. The existence of a symmetric double minimum potential with a relatively low barrier has been concluded from their experiments.

The behavior of proton in malonaldehyde is characterized by the rapid movement from one well to another in the thermal energy range. Therefore, the determination of the position of proton is a statistical or stochastic problem. In view of these circumstances, it seems to be interesting to interpret the statistical feature of proton exchange in malonaldehyde.

The purpose of the present paper is to calculate the quantum mechanical state of malonaldehyde on the basis of the CNDO/2 potential surface. The distribution of proton on the reaction coordinate and the rate of transformation between two conformers have also been calculated and discussed with relation to the temperature.

Theoretical Description of Quantum Mechanical State

In this section, we give a brief description of the quantum mechanical model for the motion of the reacting system.

Reaction Coordinate. The reaction coordinate is defined in the framework of the Born–Oppenheimer potential

$$H_{el}(r,\mathcal{R})\Phi_{el}(r,\mathcal{R}) = W(\mathcal{R})\Phi_{el}(r,\mathcal{R}) \qquad (1)$$

where H_{el} is the electronic hamiltonian, Φ_{el} is the electronic wave function, W is the Born–Oppenheimer energy, and r and $\mathcal{R}$ are the electronic and the nuclear position vectors, respectively.

Let us consider a reacting system including N atoms. At a nonequilibrium point on the reaction coordinate, the direction of displacement of nuclear configuration along the reaction coordinate is given by the use of potential energy gradients as follows:[6]

$$\ldots = \frac{M_\alpha\, dX_\alpha}{\partial W/\partial X_\alpha} = \frac{M_\alpha\, dY_\alpha}{\partial W/\partial Y_\alpha} = \frac{M_\alpha\, dZ_\alpha}{\partial W/\partial Z_\alpha} = \ldots \quad (\alpha = 1, 2, \ldots, N) \qquad (2)$$

where X_α, Y_α, and Z_α are the Cartesian coordinates of nucleus of mass M_α. The Eckart condition to fix the translation and rotation of the center of gravity[12] is automatically satisfied in eq 2:[6]

$$\sum_\alpha M_\alpha\, dX_\alpha = \sum_\alpha M_\alpha\, dY_\alpha = \sum_\alpha M_\alpha\, dZ_\alpha = 0$$

and

$$\sum_\alpha M_\alpha(X_\alpha\,dY_\alpha - Y_\alpha\,dX_\alpha) = \sum_\alpha M_\alpha(Y_\alpha\,dZ_\alpha - Z_\alpha\,dY_\alpha)$$
$$= \sum_\alpha M_\alpha(Z_\alpha\,dX_\alpha - X_\alpha\,dZ_\alpha) = 0 \quad (3)$$

Here we adopt the mass-weighted Cartesian coordinates, $x_1, x_2, \ldots, x_{3N}$, so that eq 2 is rewritten as

$$\frac{dx_1}{\partial W/\partial x_1} = \frac{dx_2}{\partial W/\partial x_2} = \ldots = \frac{dx_{3N}}{\partial W/\partial x_{3N}} \quad (2a)$$

These equations determine an infinite number of curves in the $3N$-dimensional space spanned by these coordinates. If we designate the length measured along one such curve as S, we have

$$\frac{dx_i}{dS} = \frac{\partial W/\partial x_i}{dW/dS} \quad (i = 1, 2, \ldots, 3N) \quad (4)$$

where

$$\frac{dW}{dS} = \pm\left(\sum_{i=1}^{3N}\left(\frac{\partial W}{\partial x_i}\right)^2\right)^{1/2} \quad (5)$$

The sign of eq 5 is plus for an ascending path and minus for a descending path. Such a curve which passes three equilibrium points, the initial system, the transition state, and the final system of a given reaction path, is termed an "intrinsic" reaction coordinate of that reaction.[6]

At an equilibrium point, the displacement vector in the direction of the reaction coordinate is given by one of the eigenvectors derived from the following secular equation:

$$\det\left(\frac{\partial^2 W}{\partial x_i \partial x_j} - \delta_{ij}\kappa\right) = 0 \quad (6)$$
$$(i, j = 1, 2, \ldots, 3N;\ \kappa = \text{const})$$

Among $3N$ eigenvectors, six with zero eigenvalue correspond to the translation of the center of gravity and the rotation about the center of gravity. The nuclear configuration along the reaction coordinate is obtained when we solve the simultaneous equation, eq 4, by setting the initial condition such that the solution conforms to one of the normal coordinates of an equilibrium configuration.

In order to describe the internal motion of the reacting system, we have to determine the $3N - 6$ internal coordinates. Since six redundant coordinates can be eliminated by the use of eq 3, we can define the local coordinate system $\{\xi_1(S), \xi_2(S), \ldots, \xi_f(S)\}$ at any point on the reaction coordinate, which is connected with the components of the infinitesimal displacement vector

$$dx_i = \sum_{j=1}^{f}\frac{\partial x_i}{\partial \xi_j}\,d\xi_j$$

where $f = 3N - 6$ is the internal degree of freedom. When we set $d\xi_1$ to the displacement vector along the reaction coordinate, the remaining coordinates ξ_i $(i = 2, 3, \ldots, f)$ satisfy the relation

$$\frac{\partial W}{\partial \xi_i} = \sum_{j=1}^{3N}\frac{\partial W}{\partial x_j}\frac{\partial x_j}{\partial \xi_i} = \frac{dW}{dS}\sum_{j=1}^{3N}\frac{dx_j}{dS}\frac{\partial x_j}{\partial \xi_i} = \frac{dW}{dS}\delta_{1i} \quad (7)$$

Then we can get the coordinate system $\{\xi_1, \xi_2, \ldots, \xi_f\}$ which is orthogonal to the reaction coordinate and satisfies eq 7.

Schrödinger Equation. The general form of the quantum mechanical hamiltonian can be written by the use of the coordinate system defined in the previous section as:[13,14]

$$H = -\tfrac{1}{2}g^{1/4}\left\{\frac{\partial}{\partial \xi_1}g_{11}g^{-1/2}\frac{\partial}{\partial \xi_1} + \sum_{i=2}^{f}\left(\frac{\partial}{\partial \xi_1}g_{1i}g^{-1/2}\frac{\partial}{\partial \xi_i} + \frac{\partial}{\partial \xi_i}g_{i1}g^{-1/2}\frac{\partial}{\partial \xi_1}\right) + \sum_{i,j=2}^{f}\frac{\partial}{\partial \xi_i}g_{ij}g^{-1/2}\frac{\partial}{\partial \xi_j}\right\}g^{1/4} + W(\xi_1, \xi_2, \ldots, \xi_f) \quad (8)$$

with

$$g = \det(g_{ij})$$

and

$$(g_{ij}) = (\tilde{g}_{ij})^{-1}$$

The matrix $(\tilde{g}_{ij})$ is the ordinary kinetic tensor with its elements

$$\tilde{g}_{ij} = \sum_{k=1}^{3N}\frac{\partial x_k}{\partial \xi_i}\frac{\partial x_k}{\partial \xi_j} \quad (9)$$
$$(i, j = 1, 2, 3, \ldots, f)$$

From the definition of the reaction coordinate, the kinetic tensor is diagonal on the reaction coordinate. When we expand them by a power series of the vibrational coordinates, ξ_i $(i = 2, 3, \ldots, f)$,

$$\tilde{g}_{11} = 1 + \sum_{i=2}^{f}\left(\frac{\partial \tilde{g}_{11}}{\partial \xi_i}\right)_0\xi_i$$
$$\tilde{g}_{1i} = \tilde{g}_{i1} = \sum_{j=2}^{f}\left(\frac{\partial \tilde{g}_{1i}}{\partial \xi_j}\right)_0\xi_j$$

and

$$\tilde{g}_{ij} = \delta_{ij}$$

the kinetic energy term of eq 8 is approximated to the first order of the expansion:

$$T \simeq -\tfrac{1}{2}\left[\left\{1 - \sum_{i=2}^{f}\left(\frac{\partial \tilde{g}_{11}}{\partial \xi_i}\right)_0\xi_i\right\}\frac{\partial^2}{\partial \xi_1^2} - \sum_{i=2}^{f}\left(\frac{\partial \tilde{g}_{1i}}{\partial \xi_i}\right)_0\frac{\partial}{\partial \xi_1} - \sum_{i,j=2}^{f}\left(\frac{\partial \tilde{g}_{1i}}{\partial \xi_j}\right)_0\xi_j\left(\frac{\partial^2}{\partial \xi_1 \partial \xi_i} + \frac{\partial^2}{\partial \xi_i \partial \xi_1}\right) + \sum_{i=2}^{f}\frac{\partial^2}{\partial \xi_i^2}\right] \quad (10)$$

The potential part of the hamiltonian is divided into two parts

$$W(\xi_1; \xi_2, \xi_3, \ldots, \xi_f) = W_1(\xi_1) + W_2(\xi_1; \xi) \quad (11)$$

and

$$W_2(\xi_1; 0) = 0$$

where $\xi = (\xi_2, \xi_3, \ldots, \xi_f)$. The first term of eq 11 means the change of potential energy along the reaction coordinate and the second one is that of vibrational coordinates except for the reaction coordinate. This term is approximated as the sum of the contributions of each vibrational coordinate

$$W_2(\xi_1; \xi) \simeq \sum_{i=2}^{f} W_2^i(\xi_1; \xi_i) \quad (12)$$

We now define the zeroth order vibrational hamiltonian, which corresponds to the motion perpendicular to the reaction coordinate

$$H_V = -\frac{1}{2}\sum_{i=2}^{f}\left\{\frac{\partial^2}{\partial \xi_i^2} + W_2^i(\xi_1; \xi_i)\right\} \quad (13)$$

The eigenfunction is expressed as the product of respective vibrational wave function,

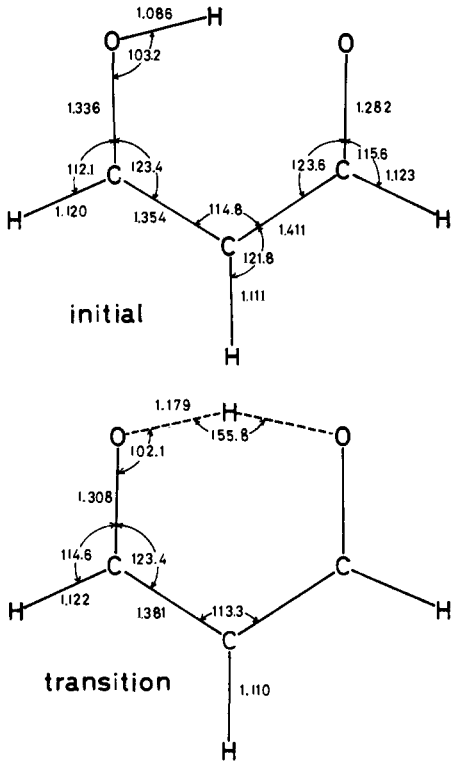

Figure 1. Optimized geometries of the initial and transition states. Bond length and angle are given in Å and deg, respectively.

$$H_V\Psi_K = E_K{}^V(\xi_1)\psi_K \tag{14}$$

and

$$\psi_K = \prod_{i=2}^{f} \chi_{K_i} \tag{15}$$

In eq 14 and 15, the suffix K represents the combination of the quantum number of respective modes. The wave function χ_{K_i} satisfies the relation

$$\left\{-\frac{1}{2}\frac{\partial^2}{\partial\xi_i{}^2} + W_2{}^i(\xi_1;\xi_i)\right\}\chi_{K_i} = \epsilon_{K_i}(\xi_1)\chi_{K_i} \tag{16}$$

and

$$E_K{}^V(\xi_1) = \sum_{i=2}^{2} \epsilon_{K_i}(\xi_1) \tag{17}$$

The wave function of the reacting system can be expanded by the vibrational wave function 15:

$$\Psi(\xi_1;\xi) = \sum_K u_K(\xi_1)\psi_K(\xi_1;\xi) \tag{18}$$

Using eq 9, 13, 14, and 18, the Schrödinger equation

$$H\Psi(\xi_1;\xi) = E\Psi(\xi_1;\xi)$$

can be written by the following coupled equation:

$$\begin{aligned}\left\{-\frac{1}{2}\frac{\partial^2}{\partial\xi_1{}^2} + W_1(\xi_1) + E_K{}^V(\xi_1) - E\right\}u_K(\xi_1) &= \frac{2}{\partial W/\partial\xi_1}\sum_{i=2}^{f}\frac{\partial^2 W}{\partial\xi_i\partial\xi_1}\langle\chi_{K_i}|\xi_i|\chi_{K_i-1}\rangle \\ &\times\left(-\frac{1}{2}\frac{\partial^2}{\partial\xi_1{}^2}\right)u_{K-1(i)}(\xi_1) \\ &+\frac{2}{\partial W/\partial\xi_1}\sum_{i=2}^{f}\frac{\partial^2 W}{\partial\xi_i\partial\xi_1}\langle\chi_{K_i}|\xi_i|\chi_{K_i+1}\rangle \\ &\times\left(-\frac{1}{2}\frac{\partial^2}{\partial\xi_1{}^2}\right)u_{K+1(i)}(\xi_1) + \text{higher order terms}\end{aligned} \tag{19}$$

where $K - 1(i)$ and $K + 1(i)$ imply to up and down one quantum number of the ith vibrational mode. The derivation of eq 19 is straightforward and is not shown here.

The vibrational adiabatic approximation is imposed by the rhs of eq 19 to be zero. The conditions where the nonadiabatic correction is important are (1) the motion along the reaction coordinate has high kinetic energy and (2) the curvature of the reaction coordinate is large, which are easily expected from eq 19. When we treat the statistical ensemble of the proton motion in the thermal region, the nonadiabatic correction can be assumed to be negligible or cancelled. Thus eq 19 is approximated as

$$\left\{-\frac{1}{2}\frac{\partial^2}{\partial\xi_1{}^2} + W_1(\xi_1) + E_K{}^V(\xi_1) - E\right\}u_K(\xi_1) = 0$$

Effective Potential for Proton Transfer

At first, we calculated the reaction coordinate for the proton exchange in malonaldehyde within the CNDO/2 approximation.

The reaction coordinate is assumed to have B_2 symmetry of the C_s point group. The geometry of the equilibrium points on the reaction coordinate was optimized by the use of the variable metric procedure of McIver and Komornicki.[15] The derivative of the potential energy was obtained by the CNDO/2 version of the SCF formalism for a system with doubly occupied orbitals[16]

$$\begin{aligned}\frac{\partial W}{\partial x_k} = \sum_{B\neq A}\left\{Z_A Z_B\frac{\partial R_{AB}{}^{-1}}{\partial x_k} - (P_{AA}Z_B\right. &+ P_{BB}Z_A - P_{AA}P_{BB})\left.\frac{\partial\gamma_{AB}}{\partial x_k}\right\} + \sum_{B\neq A}\sum_{\mu}^{A}\sum_{\nu}^{B} \\ &\times\left(2P_{\mu\nu}\frac{\partial\beta_{\mu\nu}}{\partial x_k} - \tfrac{1}{2}P_{\mu\nu}{}^2\frac{\partial\gamma_{AB}}{\partial x_k}\right)\end{aligned} \tag{20}$$

where the coordinate x_k belongs to atom A. The notation of eq 20 is the same as in the original CNDO/2 formulation of Pople et al.[7] The geometries of the initial and transition state are shown in Figure 1. The CNDO/2 optimization of geometries within C_s symmetry framework predicts that the asymmetric configuration is stable and the barrier height is 1.04 kcal/mol. The difference in the results of Schuster or Isaacson and Morokuma seems to originate from the optimization of the backbone structure. The normal coordinates of the equilibrium points were calculated as the eigenvectors of eq 6, where the second derivative of the potential energy is calculated by the numerical differentiation of the potential gradient. In eq 6, the mass of the H atom has a value of 1836.12 au. The C and O atoms are 12 and 16 times the mass of H, respectively. Figure 2 shows the relative magnitude and the direction of the displacement vectors along the reaction coordinate at the initial, transition, and final states. The reaction coordinate was calculated by the approximate form of eq 4.

$$\frac{\Delta x_i}{\Delta S} = \frac{\partial W/\partial x_i}{\mathrm{d}W/\mathrm{d}S} \tag{21}$$

Equation 21 was solved with the step size $0.05(M_H)^{1/2}$ au, where M_H is the mass of the H atom. The energy change caused by one step is about 0.1 kcal/mol. The potential energy along the reaction coordinate, $W_1(\xi_1)$, is shown in Figure 3. The initial state is located at $-0.63(M_H)^{1/2}$ au, when the point of the transition state is chosen to be zero.

The second step of the calculation is to determine the potentials for the vibrational coordinates which are perpendicular to the reaction coordinate. We calculated the normal coordinates at eight points on the reaction coordinate from $\xi_1 = -\infty$ to 0. Among 20 vibrational coordinates, the number of in-plane modes is 14 and the remainder is out-of-plane modes. It is very

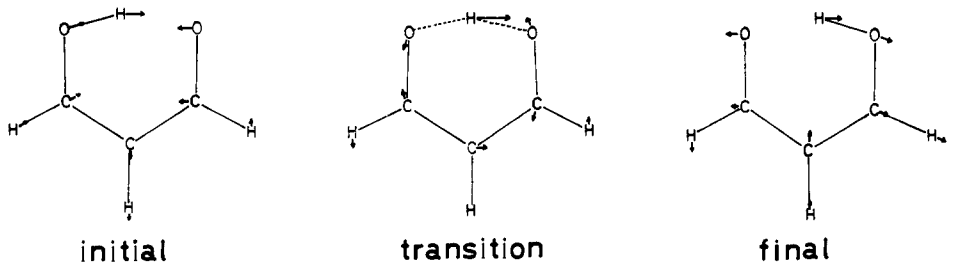

Figure 2. Displacement vectors along the reaction coordinate at three equilibrium points.

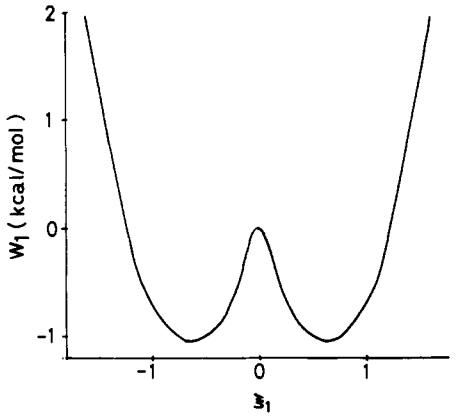

Figure 3. Potential energy profile along the reaction coordinate. The scale of reaction coordinate is $(M_H)^{1/2}$ au.

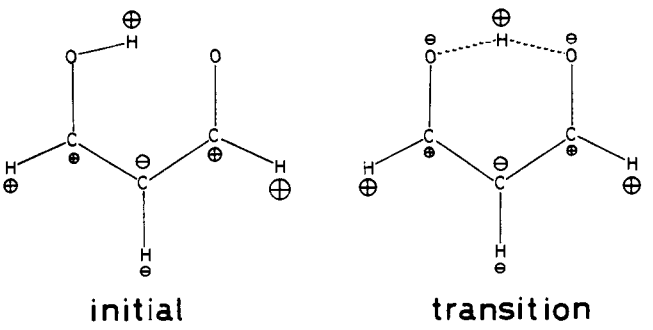

Figure 4. Displacement along one out-of-plane vibrational coordinate with a negative force constant.

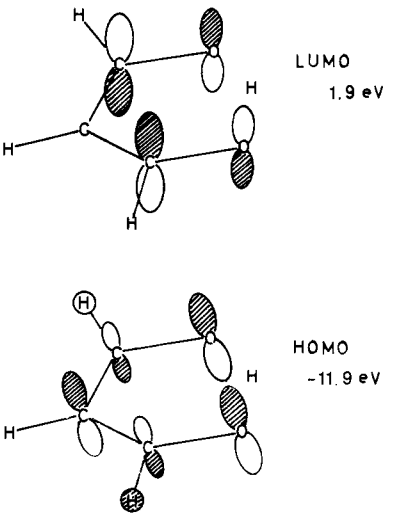

Figure 5. Schematic representation of nodal properties of HOMO and LUMO and their energies.

interesting for us that there is one out-of-plane vibrational mode with a negative force constant. The component of the displacement vector corresponding to this vibrational mode is given in Figure 4. Although malonaldehyde has been predicted to be a planar molecule in previous studies, the result of CNDO/2 calculation forecasts that the stable geometry of this molecule is nonplanar. The reason for this negative force constant is expected by the consideration of the symmetry properties of the frontier orbitals in malonaldehyde. The second order perturbation expression of force constant is given as[17]

$$\frac{\partial^2 W}{\partial \xi_i^2} = \left\langle 0 \left| \frac{\partial^2 W}{\partial \xi_i^2} \right| 0 \right\rangle + \sum_{\mathrm{I}} \frac{\left| \left\langle 0 \left| \frac{\partial V}{\partial \xi_i} \right| \mathrm{I} \right\rangle \right|^2}{E_0 - E_{\mathrm{I}}} \qquad (22)$$

where V is the sum of nuclei-electron and nuclear repulsion potentials in the electronic hamiltonian, the bra-ket is the electronic wave function, and the suffixes 0 and I imply the ground and excited states, respectively. As Bader[18] suggested, if (1) the direct product of the irreducible representation of the highest occupied (HO) MO and the lowest unoccupied (LU) MO coincides with the irreducible representation of the vibrational coordinate and (2) the transition density of these MO's is localized to the direction of the displacement vector, the second term of eq 21 plays a dominant role to reduce the force constant. Figure 5 shows the schematic representation of HOMO and LUMO at the transition state, where the above-mentioned conditions are well satisfied. This vibrational coordinate is termed as ξ_2 and the remaining coordinates as ξ_i ($i = 3, 4, \ldots, 21$). For 19 vibrational coordinates having the positive force constants, the potentials are approximated by the harmonic form

$$W_2^i(\xi_1;\xi_1) = \tfrac{1}{2} K_i(\xi_1)\xi_i^2 \qquad (23)$$

In Table I, the vibrational frequencies and assignment of them at the transition state are given. Although there is, to our knowledge, no available experimental data of vibrational spectra of malonaldehyde, the enol acetylacetone, the dimethyl derivative of malonaldehyde, has been extensively studied by means of an IR and a Raman spectroscope in both gas and liquid phases.[19] The normal coordinate analysis has alo been performed by Ogoshi and Nakamoto.[20] As seen in Table I, the CNDO/2 calculation of the vibrational frequencies somewhat overestimated on the whole, comparing with the experimental values of acetylacetone. The stretching mode shows the most serious discrepancy, which is 1.6 times the experimental values. Since the vibrational frequencies depend on the reaction coordinate, they are represented as

$$\omega_i(\xi_1) = \omega_i(0) + \Delta\omega_i(\xi_1) \qquad (24)$$

where $\omega_i(0)$ is the frequency at $\xi_1 = 0$ and $\Delta\omega_i(\xi_1)$ denotes the difference from $\omega_i(0)$. The change of vibrational frequencies with respect to the reaction coordinate, $\Delta\omega_i(\xi_1)$, is shown in Figure 6. The O-H stretching mode couples with the reaction coordinate most distinctly and changes its frequency in the process of the proton transfer.

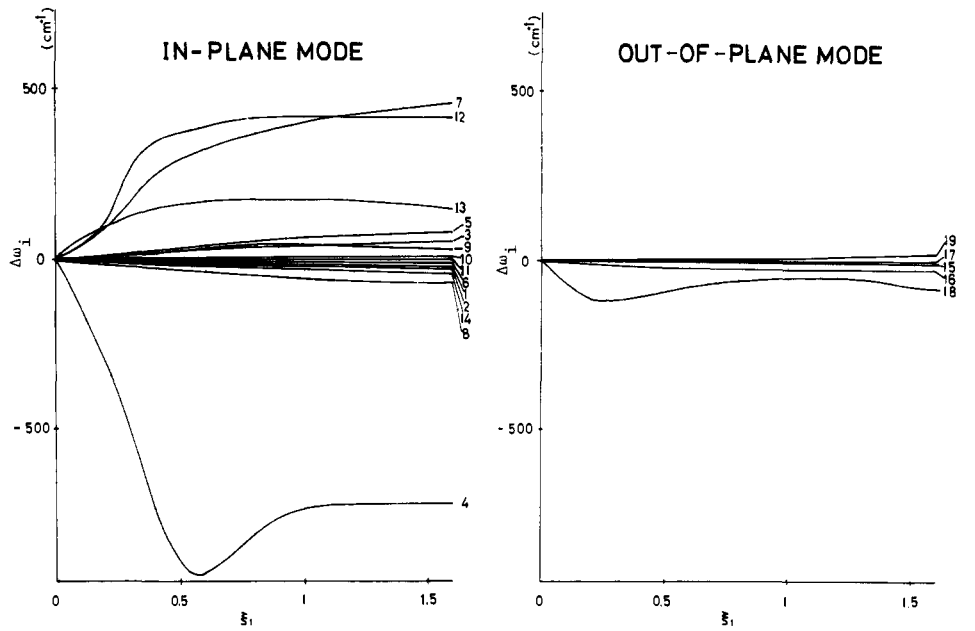

Figure 6. Change of vibrational frequencies with respect to the reaction coordinate. The number of vibrational modes is the same as in Table I. The scale of the reaction coordinate is the same as in Figure 3.

Table I. Normal Coordinates at the Transition State

No.	Freq, cm^{-1}	Symmetry	Nature of vib
		(a) In-Plane Mode	
1	4684	A_1	C-H stretching
2	4538	A_1	C-H stretching
3	4536	B_2	C-H stretching
4	3094	B_2	O-H stretching
5	2647	A_1	C-O stretching
6	2217	B_2	C-O stretching
7	2039	A_1	O-H-O bending
8	1897	A_1	C-C stretching
9	1468	B_2	C-H bending
10	1424	A_1	C-H bending
11	1280	A_1	C-H bending
12	973	A_1	Ring deformation
13	672	A_1	Ring deformation
14	572	B_2	Ring deformation
		(b) Out-of-Plane Mode	
15	1221	A_2	C-H bending
16	1186	B_1	C-H bending
17	944	B_1	O-H-O bending + C-H bending
18	791	B_1	O-H-O bending + C-C-C bending
19	358	A_2	Ring deformation

For the vibrational mode with negative force constant, ξ_2, the potential is approximated by the sixth order polynomial. The wave function is expressed by a linear combination of 20 harmonic functions

$$\chi_2(\xi_2) = \sum_{n=0}^{19} C_n N_n H_n(\alpha\xi_2) \exp(-1/2\ \alpha\xi_2^2) \qquad (25)$$

where N_n is the normalization constant and $H_n(\alpha\xi_2)$ is the Hermite polynomial. The coefficients, C_n, are determined by the variational procedure. The scaling factor, α, is optimized by the minimization of the sum of root mean square deviation of eigenvalues[21]

$$\Delta E = \sum_{m=0}^{M} (\langle m|H|m\rangle^2 - \langle m|H^2|m\rangle)^{1/2} \qquad (26)$$

where H is the vibrational hamiltonian for ξ_2 and M is chosen to be 1. The mean square error ΔE is calculated to be within 1% of the difference between the eigenvalues of the ground state and the first excited one for all values of ξ_1. In Figure 7, some lower eigenvalues of vibration ξ_2 are shown. The ground state energy is slightly below the top of the barrier at the transition state and becomes higher with distance from this point.

We can thus determine the effective potentials for the motion on the reaction coordinate

$$V_K^{\text{eff}}(\xi_1) = W_1(\xi_1) + E_K^{V}(\xi_1)$$

which is specified by the combination of the quantum number of vibrations perpendicular to the reaction coordinate

$$K = (n_2, n_3, \ldots, n_{21})$$

Figure 8 shows the effective potential for the zero-point vibration, where all vibrational quantum numbers are zero. The energy barrier height for the proton transfer reaction is lowered to 0.6 kcal/mol, and the position of the potential minimum becomes closer to the transition state, which is mainly caused by the contibution of the out-of-plane ξ_2 vibrational mode.

Statistical State of Malonaldehyde

Density Matrix. The analytical form of the effective potential along the reaction coordinate is expressed by the combination of the eighth order polynomial and one Gaussian function

$$V_K^{\text{eff}}(\xi_1) = \sum_{i=0}^{8} a_{K,i}\xi_1^{\,i} + A_K \exp(-B_K\xi_1^{\,2}) \qquad (27)$$

The parameters $a_{K,i}$, A_K, and B_K were determined by the least-squares method. The variational procedure, with 20 harmonic functions, was used to obtain the eigenvalues of them as in the case of $W_2^2(\xi_1)$. The matrix elements are easily derived by the method of Chan and Stelman.[22] The scaling factor was determined by the minimization of eq 26. The optimization was carried out to the zero-point potential in which all vibrations have zero quantum number. The same scaling factor was taken for all the effective potentials throughout. Some eigenvalues of the potential $V_0^{\text{eff}}(\xi_1)$ are shown in Figure 8. The ground state energy is slightly below the top of the barrier. The spacing of the energy spectrum differs from the case of harmonic potential. The remaining potentials have on the whole

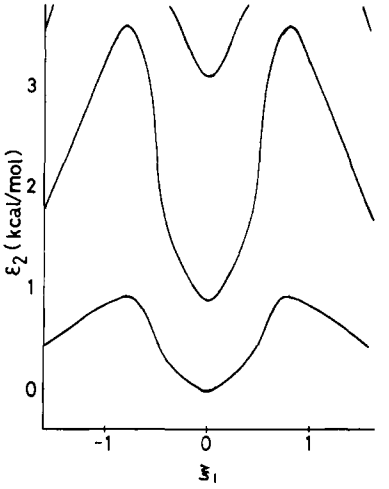

Figure 7. Change of eigenvalues for the ξ_2 vibrational mode with respect to the reaction coordinate. The scale of the reaction coordinate is the same as in Figure 3.

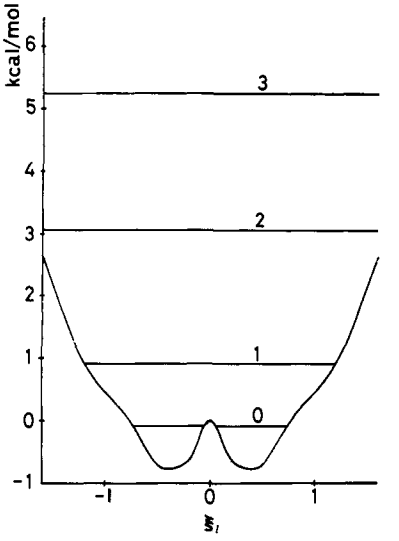

Figure 8. Profile of the effective potential $V_0^{\text{eff}}(\xi_1)$ and some lower eigenvalues for this potential. The scale of reaction coordinate is the same as in Figure 3.

a similar form of energy the level interval as $V_0^{\text{eff}}(\xi_1)$. Some of them have the ground state energy level highly bounded to the wells.

In order to describe the quantum statistical state of malonaldehyde, we have assumed the canonical ensemble in the heat bath of a given temperature. The vibrational state of the molecule is represented by the density matrix. The density matrix of the steady state is diagonal and given as

$$\rho(\xi_1,\xi) = \sum_K \sum_{m\in K} \exp(-E_{Km}/\kappa T) \times \Psi_{Km}^*(\xi_1;\xi)\Psi_{Km}(\xi_1;\xi)/Z(T) \quad (28)$$

and

$$Z(T) = \sum_K \sum_{m\in K} \exp(-E_{Km}/\kappa T)$$

where E_{Km} is the mth eigenvalues of the Kth effective potential, κ is the Boltzmann constant, T is the absolute temperature, and $Z(T)$ is the vibrational partitioning function. When we integrate eq 28 by the vibrational coordinates, ξ, we can define the density matrix on the reaction coordinate

$$\rho(\xi_1) = \int \rho(\xi_1;\xi)\, d\xi$$

$$= \sum_K \sum_{m\in K} \exp(-E_{Km}/\kappa T) u_{Km}^*(\xi_1) u_{Km}(\xi_1)/Z(T) \quad (29)$$

This density matrix implies the projection of the molecular conformer on the reaction coordinate. The projected density, $\rho(\xi_1)$, was calculated for various temperatures from 0 to 500 K, where the summation of eq 29 was truncated when the condition

$$\exp\{-(E_{Km} - E_{00})/1000\kappa\} < 10^{-4}$$

is satisfied. The calculation includes about 70 effective potentials. Figure 9 illustrates the projected density of malonaldehyde, $\rho(\xi_1)$, at 0, 300, and 500 K, respectively. As is seen in Figure 9, there exists a hollow at the middle point of the reaction coordinate, and, with the increase of temperature, it becomes deep and the density distribution is biased to the side region. This effect is easily realized by the populations of energy levels of the motion on the reaction coordinate. In Table II, the occupancies of respective energy levels at 100, 300, and 500 K are listed.[23] As the temperature increases, the contributions of the excited states become large and the first excited state plays the important role in the change of density distribution.

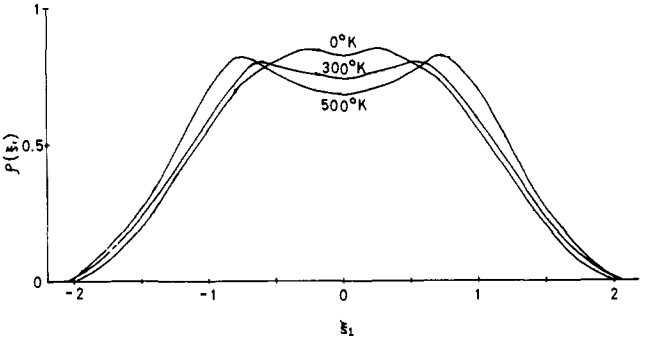

Figure 9. Density projected on the reaction coordinate at 0, 300, and 500 K. The scale of the reaction coordinate is the same as in Figure 3.

Proton Transfer Rate. In order to obtain the proton transfer rate, we have separated the conformation of malonaldehyde into two parts, which is realized by dividing the effective potential, $V_K^{\text{eff}}(\xi_1)$, at the transition state. The phenomenological expression for the proton transfer rate is given as in the conventional form:

$$\frac{dn_A(t)}{dt} = -k_{AB}(t)n_A(t) + k_{BA}(t)n_B(t) \quad (30)$$

here $n_A(t)$ and $n_B(t)$ are the population of wells A and B, $k_{AB}(t)$ is the rate from A to B, and $k_{BA}(t)$ is the rate of the reverse direction, respectively. Since the potential is symmetric, $k_{AB}(t)$ is equal to $k_{BA}(t)$. The mean rate is defined from eq 30:

$$\bar{k} = \lim_{t\to\infty} \frac{\int_0^t k_{AB}(t')\, dt'}{t} = -\lim_{t\to\infty} \frac{\ln [2n_A(t)/n_A(0) - 1]}{t} \quad (31)$$

When we define the projection operator

$$P_A = \sum_{i_A} P_{i_A} = \sum_{i_A} \phi_{i_A}\phi_{i_A}^* \quad (32)$$

the population of the well A, $n_A(t)$, is given by

$$n_A(t) = T_r(\rho(\xi_1;\xi;t), P_A) \quad (33)$$

Table II. Population of Energy Levels for the Motion on the Reaction Coordinate

Level No.	100 K	300 K	500 K
0	0.9928	0.8464	0.7289
1	0.0072	0.1495	0.2404
2	0.0000	0.0040	0.0270
3	0.0000	0.0001	0.0036
4	0.0000	0.0000	0.0001

where ϕ_{i_A} is the ith eigenfunction of the well A and $\rho(\xi_1;\xi;t)$ is the density matrix when the time is t. The eigenfunction ϕ_{i_A} is variationally determined by imposing the boundary condition that there is no amplitude in region B. The wave function is approximated by

$$\phi_{i_A}(\xi_1) = \theta(\xi_1) \times \left\{ \sum_{m=0}^{19} C_{i_A}{}^m N_m H_m(\alpha\xi_1) \exp(-\tfrac{1}{2}\alpha\xi_1{}^2) \right\} \quad (34)$$

where the normalization constant, N_m, is given as

$$N_m = \left(\frac{\alpha}{(\pi)^{1/2}\, 2^{m-1} m!} \right)^{1/2}$$

and the function $\theta(\xi_1)$ is a step function satisfying the condition:

$$\theta(\xi_1) = \begin{cases} 1 & (\xi_1 < 0) \\ 0 & (\xi_1 \geq 0) \end{cases} \quad (35)$$

The same scaling factor as in the parent double-well potential is used to calculate $\phi_{i_A}(\xi_1)$. The density matrix of the initial time is expressed by the use of the statistical operator

$$\rho(\xi_1;\xi;0) = \sum_{i_A} \phi_{i_A}\, n_{i_A}(0) \phi_{i_A}{}^* \quad (36)$$

and the initial population is given as

$$n_{i_A}(0) = T_r(\rho(\xi_1;\xi), P_{i_A}) \quad (37)$$

where $\rho(\xi_1;\xi)$ is the density matrix of steady state. The time development of the density matrix is obtained by the use of the evolution operator

$$U(t) = \exp(-iHt)$$

Then the population of the region A at the time t is calculated by

$$n_A(t) = \sum_K \left[\sum_{i,j \in K} \exp\{i(E_{Ki} - E_{Kj})t\} \times \sum_{k_A, l_A} n_{k_A}(0) S_{i,k_A}{}^K S_{j,k_A}{}^K S_{i,l_A}{}^K S_{j,l_A}{}^K \right] \quad (38)$$

where $S_{i,k_A}{}^K$ is the overlap integral

$$S_{i,k_A}{}^K = \int u_{Ki}(\xi_1) \phi_{i_A}{}^K(\xi_1)\, d\xi_1$$

In Figure 10, the time evolution of the population $n_A(t)$ is shown, in which some different features compared with the classical analogue are seen. A steady region exists where $n_A(t)$ is about 0.75, though the classical propagation is characterized by the exponential decay. The steady state is considered to originate from the interference between the wave propagating from A to B and the wave of opposite direction.

The rate of the proton transfer was calculated from eq 31. The rate is almost constant over the whole temperature range and is calculated to be $9.77 \times 10^{13}\ s^{-1}$. The activation energy of this process is nearly zero. The time interval of proton transfer from one well to another is 1.02×10^{-12} s.

The calculated result of proton transfer time implies that the movement of the hydrogen-bonded proton is very quick with the order of a low frequent molecular vibration.

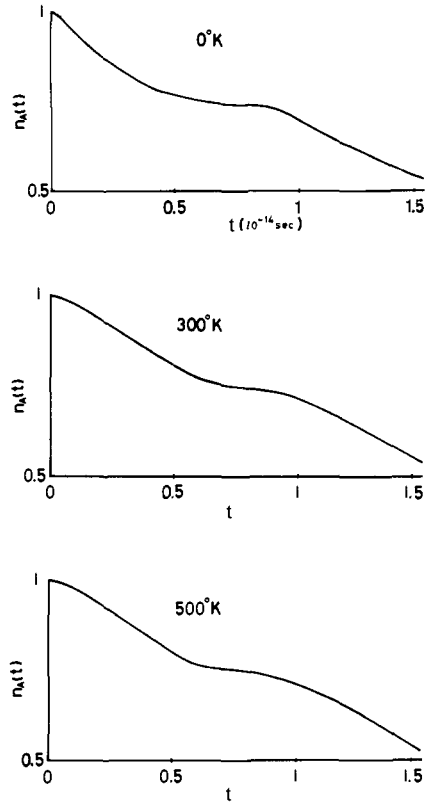

Figure 10. Time development of the population in the region A at 0, 300, and 500 K.

Discussion

Until now we have treated the dynamic behavior of the hydrogen-bonded proton of malonaldehyde by means of the "intrinsic" reaction coordinate. All vibrational motion perpendicular to the proton transfer coordinate (reaction coordinate) was taken into account. These vibrational motions were seen to affect the motion on the reaction coordinate in the case when the potential barrier is very low as in the present system compared with the usual chemical reaction where the activation barrier is moderately high.

The calculation of the vibrational state of malonaldehyde shows that the rapid transformation occurs between the two asymmetric conformers through the low potential barrier. This result is consistent with the microwave prediction of proton motion by Rowe, Duerst, and Wilson.[11] In some previous MO calculations,[8-10] the position of proton in this molecule has received much attention and different conclusions have been derived. The proton is a quantum mechanical particle and has the zero-point energy even at 0 K, so the position of the proton is a probability problem. In our statistical calculation, the distribution of the hydrogen-bonded proton on the reaction coordinate varies with the increase of temperature, and the mean position of the proton is symmetric in the low-temperature range and becomes oriented asymmetrically at the high temperature.

Our CNDO/2 calculation of the potential energy surface of malonaldehyde suggested the existence of one out-of-plane vibrational motion with a negative force constant. Then the energy minimum path for the proton has an ellipse like profile and its motion is considered to contain the orbital angular momentum. When we assumed that the vibrational frequency is proportional to the energy gap between the ground state and the first excited one, the frequencies of the motion on the mode

ξ_2 and the reaction coordinate are the same order (see Figures 7 and 8), which further convinces one of the elliptical orbital of the hydrogen-bonded proton of malonaldehyde.

Of course, the result in this paper fairly depends on the accuracy of the calculated potential energy surface. It is well known that the CNDO/2 method reproduces the bond length, bond angle, and hydrogen bond energy well. The overestimate of the C–H stretching frequencies does not affect the results, since the change of frequencies along the reaction coordinate is sufficiently small. The complete geometry optimization and the normal coordinate calculation are of advantage in the present work. It should be noted that an arbitrary displacement of out-of-plane coordinate does not lower the potential energy,[8] whereas only one of six vibrational coordinates has a negative force constant on the reaction coordinate.

Compared with the microwave spectra, the calculated potential barrier along the reaction coordinate may be underestimated. Nevertheless, we believe that the essential result obtained in the present paper will not be altered by the use of a more reliable potential surface.

The method proposed in the present paper is also applicable to any type of unimolecular reaction. The dynamic nature or the rate of unimolecular reaction is under development at the present. These works are in progress and will be presented in the near future, so this paper will be regarded as a preliminary of this series.

Acknowledgment. This work was supported by a Grant-in-Aid for Scientific Research from the Ministry of Education of Japan (No. 047068). Authors express their appreciation to the Data Processing Center of Kyoto University for generous permission to use the Facom 230-75 computer.

References and Notes

(1) R. P. Bell, "The Proton in Chemistry", Methuen and Company Ltd., London, 1959; S. Bratoz, *Adv. Quantum Chem.*, **3**, 209 (1967); G. C. Pimentel and A. L. McClellan, *Annu. Rev. Phys. Chem.*, **72**, 347 (1971).
(2) See review, P. A. Kollman and L. C. Allen, *Chem. Rev.*, **72**, 283 (1972).
(3) S. Yamabe, S. Kato, H. Fujimoto, and K. Fukui, *Bull. Chem. Soc. Jpn.*, **48**, 1 (1975); K. Morokuma, *J. Chem. Phys.*, **55**, 1236 (1971); S. Iwata and K. Morokuma, *J. Am. Chem. Soc.*, **95**, 7563 (1973).
(4) P.-O. Löwdin, *Adv. Quantum Chem.*, **2**, 213 (1965); see also, P.-O. Löwdin, *Rev. Mod. Phys.*, **35**, 724 (1963); *Biopolym. Symp.*, **1**, 161 (1964).
(5) E. A. Psehenichov and N. D. Sokolov, *Int. J. Quantum Chem.*, **1**, 885 (1967); J. Brickmann and H. Zimmermann, *J. Chem. Phys.*, **50**, 1608 (1969).
(6) K. Fukui, *J. Phys. Chem.*, **74**, 4161 (1970); K. Fukui, S. Kato, and H. Fujimoto, *J. Am. Chem. Soc.*, **97**, 1 (1975).
(7) J. A. Pople and D. L. Beveridge, "Approximate Molecular Orbital Theory", McGraw-Hill, New York, N.Y., 1970.
(8) P. Schuster, *Chem. Phys. Lett.*, **3**, 433 (1969).
(9) G. Karlström, H. Wennerström, B. Jönsson, S. Forsén, J. Almlöf, and B. Roos, *J. Am. Chem. Soc.*, **97**, 4188 (1975).
(10) A. D. Isaacson and K. Morokuma, *J. Am. Chem. Soc.*, **97**, 4453 (1975).
(11) W. F. Rowe, Jr., R. W. Duerst, and E. B. Wilson, *J. Am. Chem. Soc.*, **98**, 4021 (1976).
(12) C. Eckart, *Phys. Rev.*, **47**, 552 (1935).
(13) B. Podolsky, *Phys. Rev.*, **32**, 812 (1928).
(14) G. L. Hofacker, *Z. Naturforsh., A*, **18**, 607 (1963); J. Brickmann, *ibid.*, **28**, 1759 (1973); J. Brickmann, *J. Chem. Phys.*, **62**, 1086 (1975).
(15) J. W. McIver and A. Komornicki, *Chem. Phys. Lett.*, **10**, 303 (1971).
(16) J. Gerrat and I. M. Mills, *J. Chem. Phys.*, **49**, 1719 (1969); J. Pancir, *Theor. Chim. Acta*, **29**, 21 (1973).
(17) Although this formula is true for the exact wave function of the hamiltonian, it is valid for a qualitative discussion based on an approximate wave function.
(18) R. F. Bader, *Can. J. Chem.*, **40**, 1164 (1962).
(19) R. S. Rosmussen, D. D. Tunnicliff, and R. P. Brattain, *J. Am. Chem. Soc.*, **75**, 1068 (1947); G. G. Smith, *ibid.*, **75**, 1134 (1954); S. Bratoz, D. Hadzi, and G. Rossy, *Trans. Faraday Soc.*, **52**, 464 (1956); R. Mecke and E. Funke, *Z. Elektrochem.*, **60**, 1124 (1956); H. Musso and H. Junge, *Chem. Ber.*, **101**, 801 (1968).
(20) H. Ogoshi and K. Nakamoto, *J. Chem. Phys.*, **45**, 3113 (1966).
(21) J. Goodisman, *J. Chem. Phys.*, **47**, 5247 (1967).
(22) S. I. Chan and D. Stelman, *J. Chem. Phys.*, **39**, 545 (1963).
(23) The occupancy of the energy level n is defined by

$$\sum_K \exp(-E_{Kn}/\kappa T) \Big/ \sum_K \sum_{m \in K} \exp(-E_{Km}/\kappa T)$$

The Kinetics and Thermochemistry of the Reaction of 1,1-Difluoroethane with Iodine. The CF_2–H Bond Dissociation Energy in 1,1-Difluoroethane and the Heat of Formation of 1,1-Difluoroethyl

James M. Pickard and A. S. Rodgers*

Contribution from the Department of Chemistry, Texas A&M University, College Station, Texas 77843. *Received June 18, 1976*

Abstract: The kinetics of the gas phase reaction of 1,1-difluoroethane with iodine have been determined over the temperature range 609 to 649 K. It was found that the initial stoichiometry was consistent with the reaction $CH_3CF_2H + I_2 \rightleftharpoons CH_3CF_2I + HI$ but true equilibrium for this reaction was not obtained due to HI elimination from CH_3CF_2I which resulted in CH_3CF_2I reaching a steady state concentration at about 80 to 90% of its equilibrium value. However, kinetic data for the forward reaction obtained in the initial stages of reaction and at steady state were combined with previous results for the reverse reaction[1] to yield equilibrium constants over this temperature range from which $\Delta H_r°(298) = 12.2 \pm 0.2$ kcal/mol was obtained and $DH°(CH_3CF_2\text{–}H) = 99.5 \pm 1$ and $\Delta H_f°(CH_3\dot{C}F_2,g,298) = -72.3 \pm 2$ kcal/mol were derived. A comparison of the effects of α and β fluorine substituents on the C(sp^3)–X (X = H, I, and F) bond dissociation energies is made.

As a part of a continuing study of the effect of fluorine on bond dissociation energies, we have recently reported on the kinetics of the gas phase reaction of 1,1-difluoroiodoethane with hydrogen iodide from which we derived $DH°(CH_3CF_2\text{–}I) = 52.1 \pm 1$ kcal/mol.[1] In this study, we wish to report the kinetics and thermochemistry of the reverse reaction, namely, 1,1-difluoroethane with iodine, from which we derive values for the CF_2–H bond dissociation energy, $DH°(CH_3CF_2\text{–}H)$, and the enthalpy of formation of 1,1-difluoroethyl, $\Delta H_f°(CH_3\dot{C}F_2,g,298)$. These are the first quantitative results on the effect of α fluorine substituents in ethanes and their comparison with previous results on the effects of β fluorine